

Investigating scale effects on breach evolution of overtopped sand embankments

Mohamed Mohamed Abdellatif Mohamed*, Entesar Abdalh Soliman El-Ghorab

Hydraulics Research Institute, HRI-NWRC, Egypt

Received 21 January 2016; received in revised form 4 September 2016; accepted 13 October 2016

Abstract

The aim of this paper is to investigate the effect of scale on embankment breach processes. Relatively large scale physical models to study the embankment breach processes are expensive and time consuming. Relatively small scale experiments give better opportunity to explore the embankment breach events, but the scale effect should be considered. In this study, two small scale overtopped sand embankments were investigated in a laboratory flume. The results of these experiments are compared with the results of a previously studied large scale experiment. The analysis shows that, both the large and the small scale embankments follow almost the same embankment erodibility processes and the same rate of breach. It can be concluded that, small scale embankments can be used to study breaching events due to overtopping even with the scale effect.

© 2016 National Water Research Center. Production and hosting by Elsevier B.V. This is an open access article under the CC BY-NC-ND license (<http://creativecommons.org/licenses/by-nc-nd/4.0/>).

Keywords: Embankment breach; Sand embankment; Large scale embankment; Small scale embankment; Scale effect

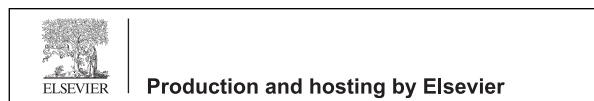
1. Introduction

It is reported that for earth/embankment dams, 35% have failed due to overtopping, 38% from piping and seepage, 21% due to foundation defects; and 6% from other failure modes (Costa, 1985). There is presently both a need and opportunity to achieve significant improvements in the technology used to analyze embankment breach processes (Wahl, 1998). The potential benefits to be achieved from this effort may significantly aid risk assessment studies, in which thresholds of embankment failure, probabilities of failure, and consequences of failure are all of prime importance (Dewey and Gillette, 1993). Unfortunately, breach simulation and breach parameter prediction have the greatest uncertainty of all aspects of embankment-breach flood forecasting (Wahl, 2001, 2004). Most approaches rely either on case studies data from past dam failures or numerical models that do not simulate the erosion mechanisms

* Corresponding author at: Hydraulics Research Institute HRI, Delta Barrage 13621, Egypt. Fax: +20 2 4 2189539.

E-mail addresses: moeg4@yahoo.com (M.M. Abdellatif Mohamed), entesar@hri-egypt.org (E.A.S. El-Ghorab).

Peer review under responsibility of National Water Research Center.



<http://dx.doi.org/10.1016/j.wsj.2016.10.003>

1110-4929/© 2016 National Water Research Center. Production and hosting by Elsevier B.V. This is an open access article under the CC BY-NC-ND license (<http://creativecommons.org/licenses/by-nc-nd/4.0/>).

and flow regimes that are relevant to a dam breach. Wahl (1998) summarized the breach parameter prediction methods and evaluated the uncertainty of predictions made using those methods.

Case studies data are especially weak for making predictions of the time needed to initiate a breach, the rate of breach formation, and the total time required for failure (Wahl, 2010). This is due to the difficulty of defining the exact point of failure and the variations in interpretation of failure by the lay person who often is the only eyewitness to a dam failure. Physically-based numerical models (e.g., NWS-BREACH) offer the potential to provide more detailed information but at this time are recognized as having limited accuracy (Wahl, 2009). Available models rely on sediment transport relations that are not applicable or are untested in the regime of flow conditions applicable to a dam breach. Furthermore, many of the available models simply do not simulate the failure mechanisms observed in case studies and laboratory tests (Wurbs, 1987; Hanson et al., 2008).

To evaluate the consequences of embankment breach and to estimate the breach outflow hydrograph and downstream flooding consequences hydraulic modeling is needed. To address questions about the embankment breach events, relatively large scale models of embankment breach are required, but the large scale experiment is relatively costly and needs longer time which will limit its ability to investigate a large number of dam breaks.

This research aims at studying the possibility of conducting embankment breach due to overtopping on relatively small scale experiments (laboratory flumes). The scale effect will be considered by comparing the results of the small scale experiments and the results collected from the previously conducted large scale experiments.

2. Model scale

Scale models of different cross sections of the embankments are built in a flume in order to simulate the overtopping of this embankment dam. To set up relevant and accurate relations between the results from the small scale model and the large scale model, the scaling is performed according to the proper similarity rules.

2.1. Similarity rules

From the hydraulic point of view, the breaching due to overtopping is a free surface process dominated by gravity phenomena. Therefore the Froude similarity must be respected. This requires that the ratio between the gravity and the inertia forces (which is the Froude number F_r) be equal in both the model and in the prototype. The Froude number is defined by Eq. (1):

$$F_r = V/(gh)^{0.5} \quad (1)$$

where F_r : the Froude number; V : the flow velocity (m/s); g : the acceleration due to gravity (m/s^2); h : the hydraulic depth (m).

Furthermore, to ensure that the viscosity effects remain insignificant, the Reynolds number must be higher than 2000 for both the model and the prototype (HRI Report 211, 2014). The Reynolds number is defined by Eq. (2):

$$Re = V R / \nu \quad (2)$$

where Re : the Reynolds number; R : the hydraulic radius (m); ν : kinematic viscosity (m^2/s).

The Reynolds number in this model is about 3000 which ensures a turbulent flow and the viscosity effect is insignificant. Important scaling ratios for Froude-scaled models are the following:

$$Q_r = L_r^{2.5} \quad (3)$$

$$V_r = L_r^{0.5} \quad (4)$$

$$t_r = L_r^{0.5} \quad (5)$$

where Q_r : the discharge scale ratio; L_r : the model length scale ratio; V_r : the velocity scale ratio; t_r : the time scale ratio.

2.2. Scaling material properties

The second consideration for model design is the selection of model working fluids and sediment materials. The working fluid for these models will be water, so fluid properties of model and prototype fluid are essentially the same,

Table 1
Description of the experiments.

Embankment No.	Type of model	Dimensions					Scale ratio	Remarks
		W (m)	H (m)	T (m)	S ₁	S ₂		
1	Large scale	5.0	1.80	1.50	2.5	2.5	1:1	Base case
2	Small scale	1.0	0.90	0.75	2.5	2.5	1:2	Test 1
3	Small scale	1.0	0.45	0.375	2.5	2.5	1:4	Test 2

W: width of the embankment (m).

H: height of the embankment (m).

T: top width of the embankment cross section (m).

S₁: side slope of the embankment facing the river.

S₂: side slope of the embankment facing the land.

ignoring minor differences caused by temperature and water quality variation. The prototype sediment is pure sand for both the large and the small scale models.

Wahl and Lentz, (2011) stated that in models that simulate sediment transport, scaling of the geometric size of model sediment is important, but for embankment breach model it is believed that the embankment erosion rates are limited by sediment detachment processes, rather than sediment transport processes. The widely accepted model for sediment detachment according to Hanson and Cook (2004) is as follows:

$$\varepsilon = k_d (\tau - \tau_c) \quad (6)$$

where ε = volume of material removed per unit surface area per unit time (m/s); τ = applied shear stress (N/m²); τ_c = critical shear stress needed to initiate sediment detachment (N/m²); k_d = detachment rate coefficient (units of length per time per stress).

If the model scale can be kept sufficiently large so that this sediment detachment model will apply to both the model and prototype, then the scale ratios for these parameters can be shown to be as in Eqs. (7) and (8):

$$\tau_r = L_r \quad (7)$$

$$k_{d,r} = L_r^{-0.5} \quad (8)$$

The critical shear stress for most embankment materials is relatively low in comparison to the applied stresses (τ), so it is often assumed to be zero in the prototype (Hanson et al., 2010). To satisfy the scaling ratio above, the critical shear stress for the model material should be reduced from the prototype value by the length scale ratio, but if the prototype value is zero, the model value can also be set to zero.

To obtain scalable model performance, the (k_d) value of the model material should be larger (more rapid erosion) than the k_d value of the large scale embankment material, and the critical shear stress should be smaller (again, more erodible). Hanson et al. (2010) provided an estimate of (k_d) based for ranges of % clay, wet and dry optimum water content and compaction effort.

2.3. Hydrodynamic considerations

The worst-case scenario simulation is when a canal embankment breached so rapidly, operational response was so delayed, or the canal was so long that the breach process was unaffected by the length of the reach or by operational response (Dun, 2007). In such a scenario, the water surface elevation in the canal would remain constant during the breach initiation and breach development processes.

2.4. Experimental condition

The large scale model test is a base case for comparison and it was done earlier by El-Ghorab et al. (2013). The other two tests for small scale experiments were carried out in this research. As can be seen in Table 1, the large scale embankment is 1.8 m high. The width at the crest is 1.5 m and with side slopes of 1:2.5. For the small scale experiment, the first embankment is 0.90 m high with top width of 0.75 m and side slopes of 1:2.5. The second embankment is

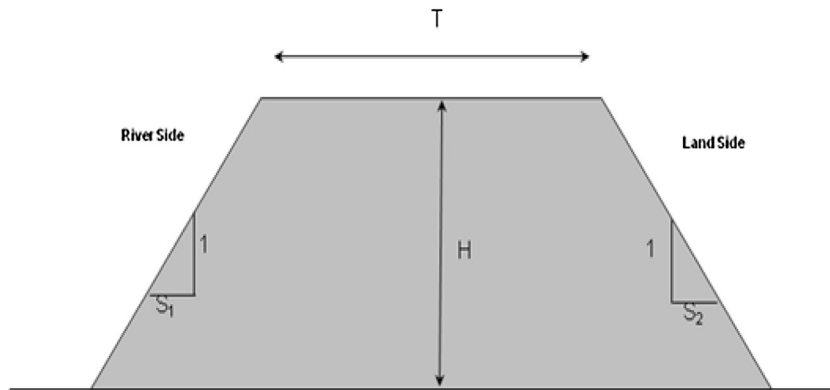


Fig. 1. Breached embankment dimensions.

0.45 m high and top width of 0.375 m with the same side slopes as the first embankment. Fig. 1 shows a depiction of the breach embankments.

3. Description of the experiments

This study focuses on conducting small scale experiments for the embankment breach and comparing the results of these experiments with the results of the previously investigated large scale experiment. Conducting embankment breach on small scale experiments (laboratory flumes) allows for more detailed investigations. The tested embankment should be compacted using the modified proctor compaction procedure for small dams. Laboratory tests of the soil would be necessary in order to obtain the necessary field compaction parameters: maximum dry unit weight and optimum water content. The parameters should be obtained following the ASTM (2003).

3.1. Large scale experiments

The selected embankment dimensions for the large scale experiment represent approximately half of typical emergency embankments (ASCE/EWRI, 2011). It is worthwhile to mention that the sand that was used in the large scale experiment as the only embankment material is the same as the sand that will be used to shape the small scale embankments but with different water content. The maximum dry density for the large scale embankment of the used sand is 2.04 gm/cm^3 while the optimum moisture content (OMC) is 8.5%. The large scale model and all data and analysis of this test can be seen (El-Ghorab et al., 2013; HRI Report 106, 2014).

3.2. Small scale experiments

These experiments involve breaching of homogenous embankments which are constructed using different dimensions. The selected embankment dimensions represent approximately 1:2 and 1:4 scales of the large scale model, Table 1.

3.3. Experimental set up

The experiments are carried out in a 30 m long flume. The most important requirement is maintaining a close to constant water surface level upstream embankment head during the breach process. A constant head during tests near the embankment is maintained by adding a reservoir in the upstream side of the flume, and adjusting the inflow rate. The breach is initiated by carving a small pilot channel at the middle of the embankment crest. The water level at various locations is monitored by a number of ultrasonic surface profilers. Once the embankment failure is complete, the breach is surveyed in detail. The flow rate downstream of the reservoir is passed through a stilling basin with a sharp-crested weir in order to measure the flow rate. Two measuring bridge profilers provided with labeled rods are deployed over the downstream face of the embankment in order to record the growth of the breach depth during the

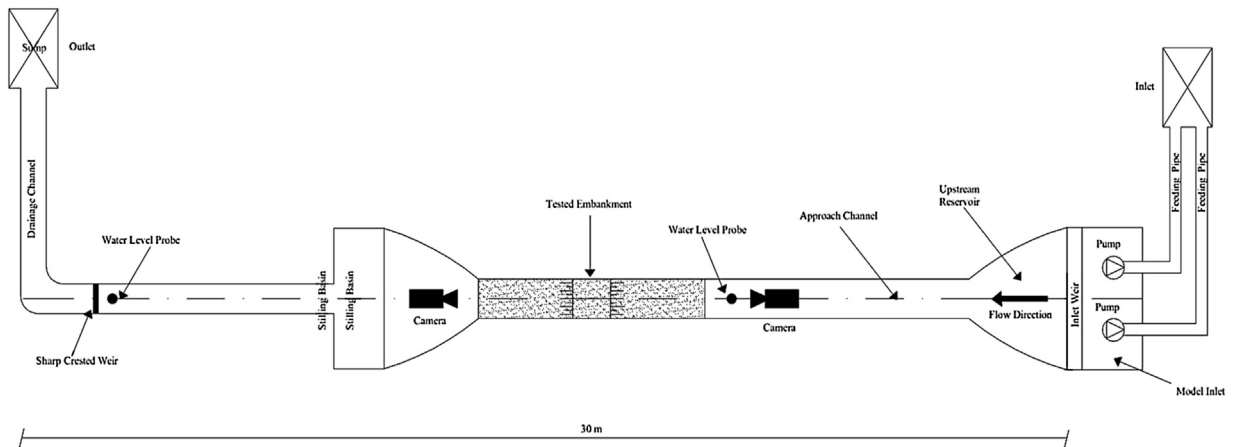


Fig. 2. Layout of the experimental flume to test the sand embankment breach.

experiment. Two high definition digital cameras with high resolution and speed are used to measure the breach width and depth evolution. The breach width evolution was directly measured by taking snapshots of the experiment recorded at regular intervals. Fig. 2 shows the experimental setup along with instrumentation. Two pumps, with a maximum combined flow capacity of 300 l/s, are used to supply water to the flume during the experiments. Fig. 3(a,b) shows part of the flume while, the labeled rods and the sand embankment are shown in Fig. 3(c,d).

3.4. Embankment material

The breach embankment is constructed from pure sand. The results of the sieve analysis for the used sand are plotted. Fig. 4 shows the grain size distribution of pure sand. The mean particle size of the sand is 0.503 mm. A sample of the sand that is used for the model construction was investigated by the soil mechanics laboratory of the Construction Research Institute, CRI in Egypt to determine the optimum moisture content and maximum dry density for the sample, Fig. 5. This data is used to amass the embankment in 6 layers for compaction. Modified proctor compaction tests are conducted for each layer to attain the maximum compaction. The optimum moisture content is 12% and the maximum dry density of the sand sample is 1.79 gm/cm³.

The water content of the sand soil that was used to form the small scale embankment was adjusted to obtain the erodibility of the sand embankment as described by Eq. (6). The method to adjust the erodibility is well explained by Hanson et al. (2010). The erodibility for the large scale model material which is pure sand is around 50 cm³/N-s. According to Eq. (8), the 1:2 scale model, the erodibility is taken as 70 cm³/N-s and in the 1:4 scale model the erodibility is taken as 100 cm³/N-s.

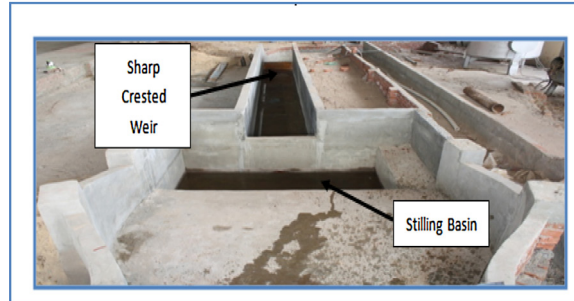
4. Test procedure

As the model design was described in detail and different applied techniques and devices for measuring the inflow and outflow as well as the water surface levels was illustrated, some information about the testing procedure is introduced below. As any of the tested embankments is assembled, the following testing procedure is carried out:

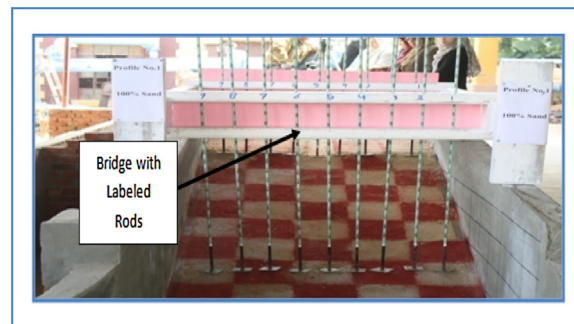
- Location of the overtopping water flow over the tested embankment is initiated by carving a small pilot channel at the middle of the embankment crest. This channel was 0.10 m wide and only 0.03 m deep. The two side slopes of such pilot channel are adjusted following the angle of repose of the embankment materials.
- The two measuring wooden bridges are installed perpendicular to the flow direction. The first one is installed on the top end of the downstream face of the tested embankment. While the other one of the wooden bridge is installed on the half distance of the downstream face of the tested embankment.
- The stilling basins and the approach channel that are located upstream of the sharp crested weir are filled with water up to the crest level of the weir.



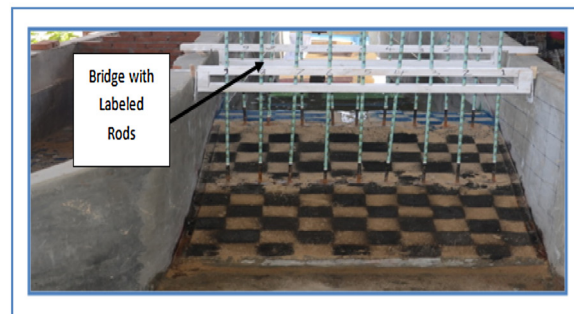
(a): The Upstream of the Flume



(b): The Downstream of the Flume



(c): The 1:2 Sand Embankments



(d): The 1:4 Sand Embankments

Fig. 3. Part of the flume, labeled rods, and the sand embankments.

- The ultra sonic sensors used inside the upstream reservoir and in the approach channel upstream of the sharp crested weir are employed to record the zero readings for the surface water levels in both sites.
- The two feeding pumps are operated to fill the upstream reservoir with water at about 20l/s. This is carried out in steps of 10 cm high each up to about 10 cm lower than the crest level of the tested embankment. The top layer is filled with lower flow rate of about 10l/s.

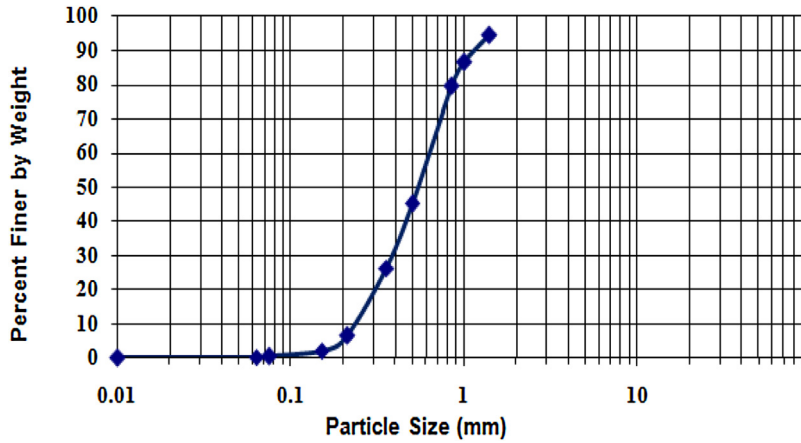


Fig. 4. The grain size distribution of the sand sample.

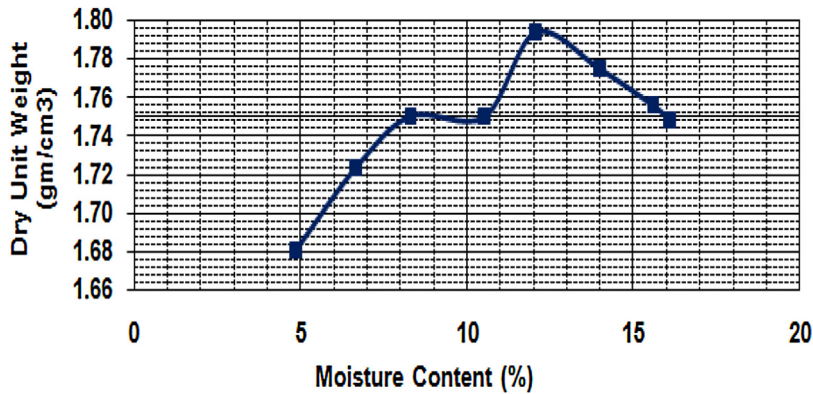


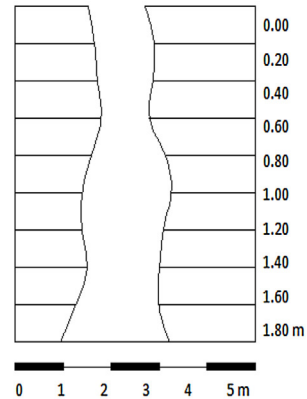
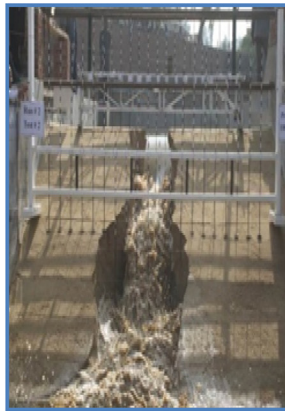
Fig. 5. Changes in dry unit weight, γ_d , as a function of moisture content for modified proctor compaction test specimens.

- The starting time for embankment breach process was then assigned as that moment when the flow is over topping the tested embankment and reaching the downstream crest level.
- The most important requirement for the model is maintaining a close to constant head during the breach process. This is fulfilled by increasing the feeding flow rate in such a way as to maintain constant water level along the whole testing duration. Each of the time and the increase in the feeding discharge is recorded up to the end of the test.
- The embankment breach process is instantaneously recorded using a high quality camera which is fixed at a suitable location downstream of the constructed embankment.
- The failure stage is reached when the water surface level in the upstream reservoir cannot be maintained even after increasing the inflow discharge to the maximum capacity for the two feeding pumps.

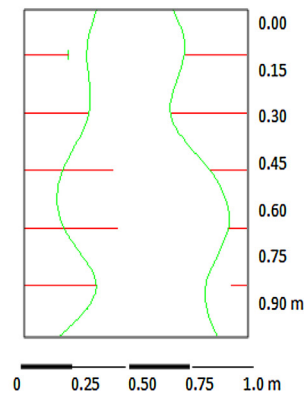
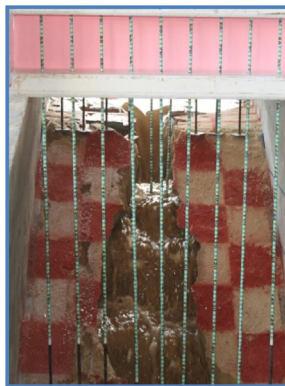
5. Experimental results

5.1. Embankment erodibility

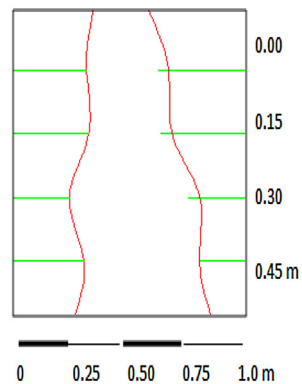
The erodibility of compacted soils is an important parameter for determining the anticipated performance of an earthen embankment during overtopping. As the flow passes the pilot channel on the top of the embankment, breach channel is formed on the downstream face of the embankment. After that, the breach channel is getting wider at its downstream end. Tractive shear stress and turbulence will cause breach failure to change from primarily vertical erosion to predominantly lateral erosion occurring along the breach channel side slopes. Undermining of the breach channel side slopes causes large volumes of unsupported material to collapse into the center of the channel and be transported further downstream. Under the action of upstream static water force and the dynamic flow drag force, some part of



a: Large Scale Sand Embankment (Base Case)



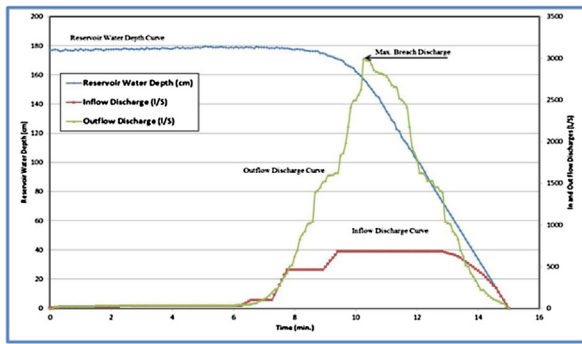
b: Small Scale Sand Embankment (1:2)



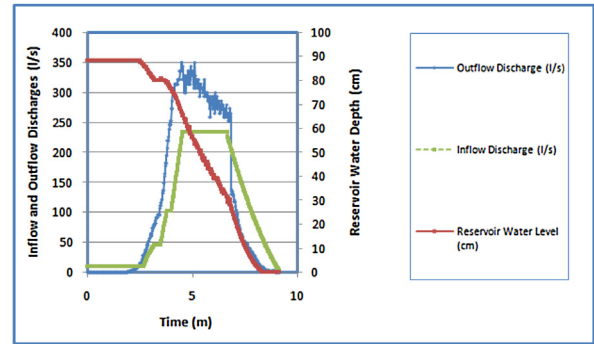
c: Small Scale Sand Embankment (1:4)

Fig. 6. Snap shots for the head-cut erodibility of large and small scale embankments.

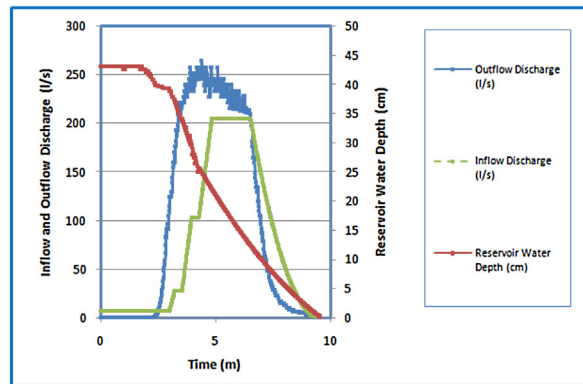
soil near the upstream entrance of the breach channel may lose its stability and suddenly collapse. Fig. 6a shows the formation of the failure shape in the large scale embankment just before collapse and it took 7.24 min to reach this shape. Fig. 6b shows the formation of the failure shape before collapse to the 1:2 small scale embankments and it took almost 5.11 min to occur. The failure shape before sudden collapse in the 1:4 small scale embankment is shown in



(a): Hydrograph, Water level, and Inflow Discharge of the Large Scale Embankment (El-Ghorab et al., 2013)



(b): Hydrograph, Water level, and Inflow Discharge of the 1:2 Small Scale Embankment



(c): Hydrograph, Water level, and Inflow Discharge of the 1:4 Small Scale Embankment

Fig. 7. Hydrograph, water level, and inflow discharge for the large and small scale sand embankments.

Table 2
Hydrograph characteristics of the sandy embankment breach.

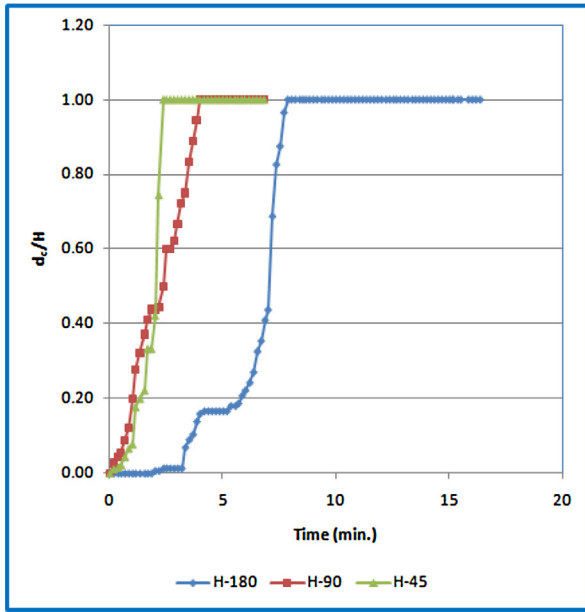
Embankment No.	Peak flow (l/s)	Time to peak flow (min)
1	2750	10
2	350	4.5
3	250	4.0

Fig. 6c and it took about 3.6 min to occur. It can be seen in Fig. 6(a–c) that the three embankments take almost the same shape before sudden collapse occurs but with different times due to the scale effect.

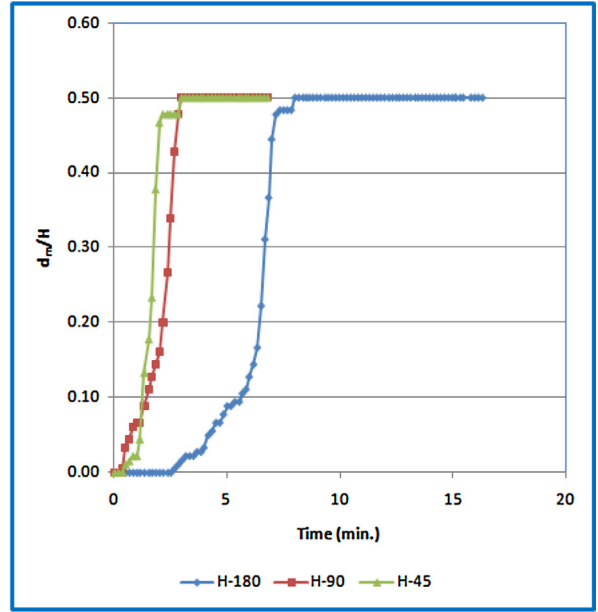
5.2. Breach temporal evolution

5.2.1. Breach hydrograph

It can be realized during the experiment that, the upstream water level of the reservoir decreases in spite of an increase in the inflow to the reservoir. Fig. 7(a–c) presents the hydrograph, water level, reservoir inflow of the tested large and small scale embankments. Table 2 shows the peak discharges, and the time to reach the peak flow. The flow hydrographs for the large and the small scale embankments behave the same way. It increases gradually with the breach development till it reaches a maximum value then it decreases till it reaches zero with a complete failure of the embankment.

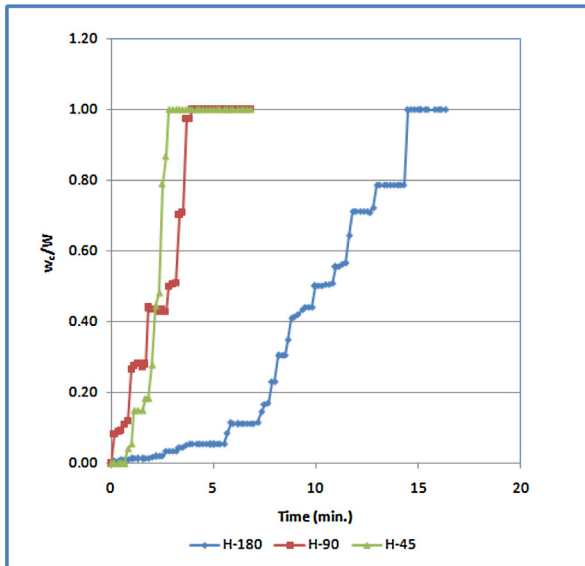


(a): Breach Depth at the Crest

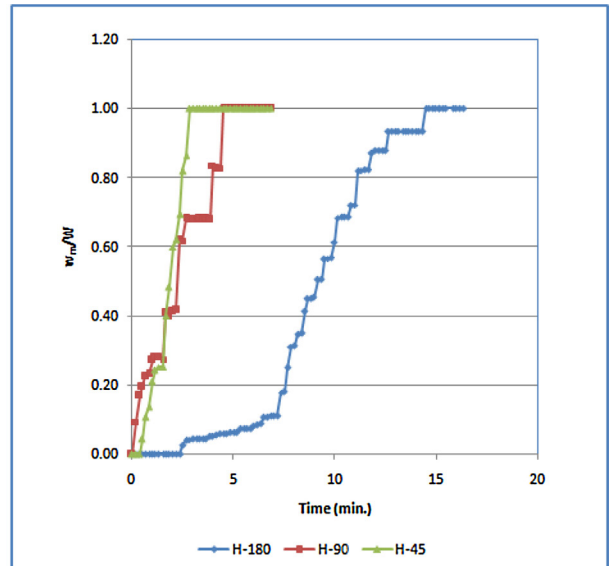


(b): Breach Depth at the Middle

Fig. 8. Normalized breach depth at the crest and the middle of the downstream face of the embankment.



(a): Breach Width at the Crest



(b): Breach Width at the Middle

Fig. 9. Normalized breach width at the crest and the middle of the downstream face of the embankment.

Figs. 8 and 9(a,b) show the normalized breach depth and width at the crest and the middle of the downstream face of the sand embankments respectively. The breach depth (d) is divided by the height of the embankment (H), and the breach width (w) is divided by the width of embankment (W). The results show that in the sand embankment, the crest is severely eroded within a few minutes due to the loss of supporting material, which resulted from head cut in the upper part of the downstream face of the embankment. It is clear from Figs. 8 and 9 that the erosion mechanism of the large scale embankment (H-180), the 1:2 small scale embankment (H-90), and the 1:4 small scale embankment

Table 3
 Maximum rate of breach width and depth at the crest of the embankment.

Rate (cm/s)	Embankments			Average
	1	2	3	
Rate of breach width (cm/s)	0.51	0.53	0.55	0.53
Rate of breach depth (cm/s)	0.38	0.35	0.36	0.36

Table 4
 Maximum rate of breach width and depth at the middle of the embankment.

Rate (cm/s)	Embankments			Average
	1	2	3	
Rate of breach width (cm/s)	0.60	0.58	0.59	0.59
Rate of breach depth (cm/s)	0.21	0.22	0.24	0.22

(H-45) is almost the same even though the breach process is faster in the small scale embankment than the large scale embankment. In the small scale embankments the breach starts at shorter time than the large scale embankments. This is because the scale difference between the large and the small scale embankments.

5.2.2. Rate of breach

The rate of breach is obtained by dividing the maximum breach width or the maximum breach depth by the total breach time. Tables 3 and 4 show the maximum rate of breach width and depth for the large and small scale sand embankments at the crest and the middle of the downstream face of the embankment respectively. It can be seen that the results of the average rate of breach width and breach depth at the crest of the downstream face of the embankment are 0.53 cm/s and 0.36 cm/s respectively. At the same time, the average breach width and breach depth at the middle of the downstream face of the embankment are 0.59 cm/s and 0.22 cm/s respectively. It can be realized that the rate of breach width is higher in the middle than in the crest of the embankment, while the opposite occurs for the breach depth rate. This is because the erosion of the breach channel initially proceeds with the invert slope parallel to the slope of the downstream face of the embankment. After the downstream toe of the breach channel invert has eroded upstream to a pivot point along the base of the embankment, the channel invert slope then starts to flatten while rotating about this fixed (pivot) point. As erosion continues, the channel invert slope reduces to a terminal value of minimum slope, the channel subsequently widening with a central flatbed region. This explains why the rate of breach width is higher in the middle of the embankment than its crest. The embankment crest is severely eroded within a few minutes due to the loss of supporting embankment material, which resulted from head-cut in the upper part of the downstream embankment surface; this explains why the rate of breach depth is higher in the crest of the embankment (Coleman et al., 1997).

6. Conclusions

A comprehensive experimental investigation to study the scale effects on the embankment breach process in sand embankments has been presented. It can be concluded from this study that, even though full-scale and large scale tests are vital for better understanding of the breach mechanism in sand embankments, they are expensive and time consuming. This might limit the ability of such type of tests to study large numbers of embankment breach. Relatively small scale experiments (laboratory flumes) represent good opportunity to study the embankment breach phenomenon in detail but the scale effect should be considered. Two different small scale sand embankments were tested in this study. These small scale embankments represent one meter strip of a previously studied large scale embankment. The small scale model is based on Froude similarity and sediment detachment rules. The cross sections of the first and second small scale sand embankments are of scale 1:2 and 1:4 respectively. The study shows that the large and the small scale embankments follow the same erodibility process. Also, the large and the small scale experiments pursue almost the same rate of breach. It was realized that the rate of breach width is higher in the middle than in the crest of

the embankment, while the opposite occurs for the breach depth rate. Also, in the small scale embankments the breach starts at shorter time than the large scale embankments. This is because of the scale difference between the large and the small scale embankments. It can be concluded from this study that the small scale experiment can be used to study the overtopping breach for sand embankments even with some scale effects. As the primary purpose of this study was to determine the performance of small scale embankments to represent embankment breach processes; after the first set of experiments, the complexity of the structure became increasingly apparent. Therefore, it is recommended for future research to expand these experiments with different types of soils and different soil mixtures (e.g., sand, silt and clay soils).

Conflict of interest

None.

Acknowledgments

This study was supported by the National Water Research Center (NWRC), Egypt as part of a larger study devoted toward evaluating the scale effects on dam breach. This support is gratefully acknowledged. This work was carried out in the Hydraulics Research Institute (HRI), Delta Barrage, Egypt. The authors gratefully acknowledge the collaboration and effort done by all staff members of the Institute. Their contribution to the experimental study is appreciated.

References

- ASCE/EWRI, 2011. Task committee on dam/levee breaching, earthen embankment breaching. *J. Hydraul. Eng.* 137 (2), 1549–1564.
- ASTM, 2003. *Annual Book of ASTM Standards, Section 4: Construction, Vol. 04.08.* ASTM, Philadelphia.
- Coleman, S.E., Jack, R.C., Melville, B.W., 1997. Overtopping breaching of noncohesive embankment dams. In: *Energy and Water: Sustainable Development.* ASCE, pp. 42–47.
- Costa, E., 1985. *Floods from Dam Failures.* U.S. Geological Survey, Open-File Report. No. 85-560, Denver.
- Dewey, R.L., Gillette, D.R., 1993. Prediction of embankment dam breaching for hazard assessment. In: *Proceedings of ASCE Specialty Conference on Geotechnical Practice in Dam Rehabilitation,* Raleigh, North Carolina, April 25–28.
- Dun, R.W.A., 2007. An improved understanding of canal hydraulics and flood risk from breach failures. *J. Water Environ.* 21 (1), 9–18.
- El-Ghorab, E.A., Fahmy, A., Fodda, M., 2013. Large scale physical model to investigate the mechanics of embankment erosion during overtopping flow. *Eng. Res. J.* 36 (3), 287–301.
- HRI, 2014a. *Hydraulics Research Institute, Report No. 106.* In: *Embankment Failure and Levee Breach: Testing Results for Model Nos. 1, 3, 7, and 8.* Hydraulics Research Institute, HRI, Cairo, Egypt.
- HRI, 2014b. *Hydraulics Research Institute, Report No. 211.* In: *Scale Effects of Dam Breach Experiments.* Hydraulics Research Institute, HRI, Cairo, Egypt.
- Hanson, G.J., Cook, K.R., 2004. Apparatus, test procedures, and analytical methods to measure soil erodibility in situ. *J. Appl. Eng. Agric.* 20 (4), 455–462.
- Hanson, G.J., Tejral, R.D., Temple, D.M., 2008. Breach parameter and simulation comparisons. In: *Proceedings of the Annual Conference of Association of State Dam Safety Officials (ASDSO),* Indian Wells, California, September 7–11.
- Hanson, G.J., Wahl, T.L., Temple, D.M., Hunt, S.L., Tejral, R.D., 2010. Erodibility characteristics of embankment material. In: *Proceedings of the Annual Conference of Association of State Dam Safety Officials (ASDSO),* Seattle, WA—September 19–23.
- Wahl, T.L., 1998. *Prediction of Embankment Dam Breach Parameters: A Literature Review and Needs Assessment,* Dam Safety Research Report DSO-98-004. U.S. Dept. of the Interior, Bureau of Reclamation, Denver, Colorado.
- Wahl, T.L., 2001. The uncertainty of embankment dam breach parameter predictions based on dam failure case studies. In: *Proc. USDA/FEMA Workshop: Issues, Resolutions, and Research Needs Related to Embankment Dam Failure Analysis,* CD-ROM, Oklahoma City, Okla: USDA/FEMA.
- Wahl, T.L., 2004. Uncertainty of predictions of embankment dam breach parameters. *J. Hydraul. Eng.* 130 (5), 389–397.
- Wahl, T.L., 2009. Evaluation of new models for simulating embankment dam breach. In: *Proceedings of the Annual Meeting of the Association of State Dam Safety Officials (ASDSO),* Hollywood, FL, September 27–October 1.
- Wahl, T.L., 2010. Dam breach modeling—an overview of analysis methods. In: *Proceedings of the Joint Federal Interagency Conference on Sedimentation and Hydrologic Modeling,* Las Vegas, NV, June 27–July 1.
- Wahl, T.L., Lentz, D.J., 2011. *Physical Hydraulic Modeling of Canal Breaches.* U.S. Dept. of the Interior, Bureau of Reclamation, Technical Service Center, 86-68460, Denver, CO 80225.
- Wurbs, A.R., 1987. Dam-breach flood wave models. *J. Hydraul. Eng.* 113 (1), 29–46.